CHANDRA
X-ray Center 60 Garden St., Cambridge Massachusetts 02138 USA

MEMORANDUM

Date: November 1, 2014
From: **Ping Zhao**
To: **CXC**
Subject: **Chandra Optical Axis, Aimpoint and Their Drifts**
File: `oxap_memo.tex`
Version: `2.0`

Chandra X-ray Observatory revolutionized the X-ray astronomy as being the first, and so far the only, X-ray telescope achieving sub-arcsecond resolution. Chandra comprises of three principal elements: the High Resolution Mirror Assembly (HRMA), Pointing Control and Aspect Determination (PCAD) system, and the Science Instrument Module (SIM). To achieve and retain the unprecedented imaging quality, it is critical that these three principal elements stay rigid and stable for the entire life time of the Chandra operation. Measuring and tracking the telescope optical axis and aimpoint positions are the key to understand the stability of the telescope and to maintain the optimal Chandra operation.

1 Definitions

Let's first give the following definitions:

- Focal-Point: Point on the focal plane where the sharpest PSF is located.

- Optical Axis: Axis perpendicular to the focal plane at the focal-point.

- Aimpoint: Point on the focal plane where the image of a source with zero Y and Z offsets is located.

For ideal Wolter-I mirror pairs, the optical axis is the mathematical axis of both paraboloid and hyperboloid mirror surfaces, and it passes through both focal-point and aimpoint on the focal plane, i.e. the focal-point and aimpoint are the same point. For the actual HRMA, the focal-point and aimpoint are close but not identical. The origin of the Y and Z offsets was set before the Chandra launch, with the best estimate at the time for the aimpoint and optical axis positions. This origin has never been changed. The actual aimpoint and optical axis were never at the location of the pre-launch origin. Their positions have been changing continuously since the Chandra launch. This memo discusses their drifts, its impact to the Chandra operation and corresponding adjustment made.

2 Telescope Pointing

The telescope pointing, i.e. the target acquisition, is accomplished through the following steps, as illustrated by Figure 1 (refer POG Figure 5.3):

1. Target coordinate: the target coordinate is requested by the observer, which is registered as (RA_targ, Dec_targ) in the data header.
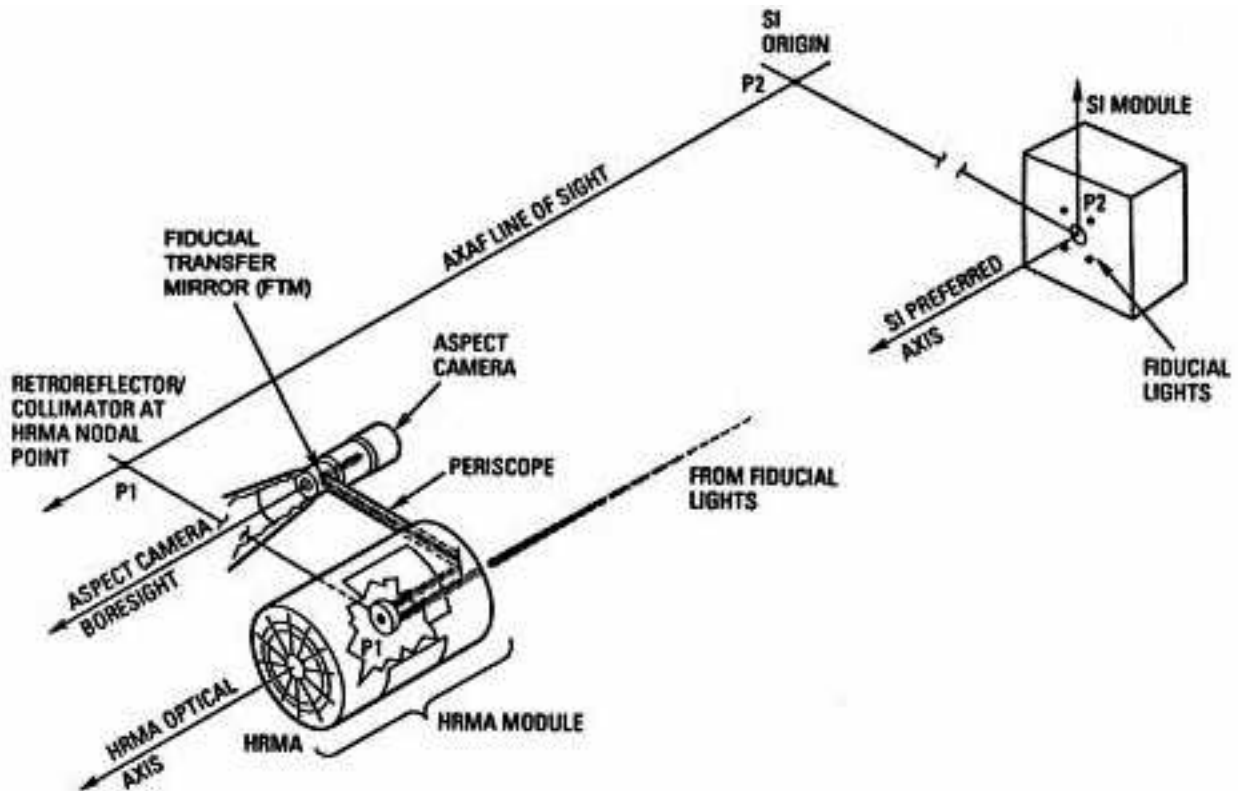
Figure 1: Chandra Pointing and Fiducial Transfer System. (POG: Figure 5.3.)

2. ACA attitude (Aspect Camera Assembly pointing): based on the target coordinate (RA_targ, Dec_targ), the ACA pointing (command position) is computed in terms of quaternions, which are registered in the ACA database. There is an $89.6''$ offset between the target position and ACA pointing, due to the pre-launch ACA alignment.

3. Telescope attitude (HRMA pointing): once the ACA is pointed to its command position, the HRMA is automatically pointed to (RA_pnt, Dec_pnt), which is the computed mean pointing of the (dithered) observation. This information is registered in the data header. There is a $\sim 97''$ offset between the HRMA pointing and the ACA pointing.

4. Target position: once the HRMA is pointed to (RA_pnt, Dec_pnt), the image of an on-axis target will be at the aimpoint[1], which has the observer requested coordinates (RA_targ, Dec_targ). There is a $\sim 17''$ offset between (RA_pnt, Dec_pnt) and (RA_targ, Dec_targ).

---

[1]Since the Chandra spacecraft has a built-in dither (of Lissajous figure with peak-to-peak amplitude of $16''$ for ACIS and $40''$ for HRC) on its pointing position to average across calibration uncertainties, the aimpoint is actually the center of the dither pattern.

3   Aimpoint on Chandra Detectors

For each Chandra observation, one of four Chandra detectors is aligned with the HRMA optical axis by moving the entire SIM to that detector's nominal SIM-Z position. Figure 2 shows the Chandra detectors layout in the SIM plane and the aimpoint locations with their nominal SIM-Z positions.
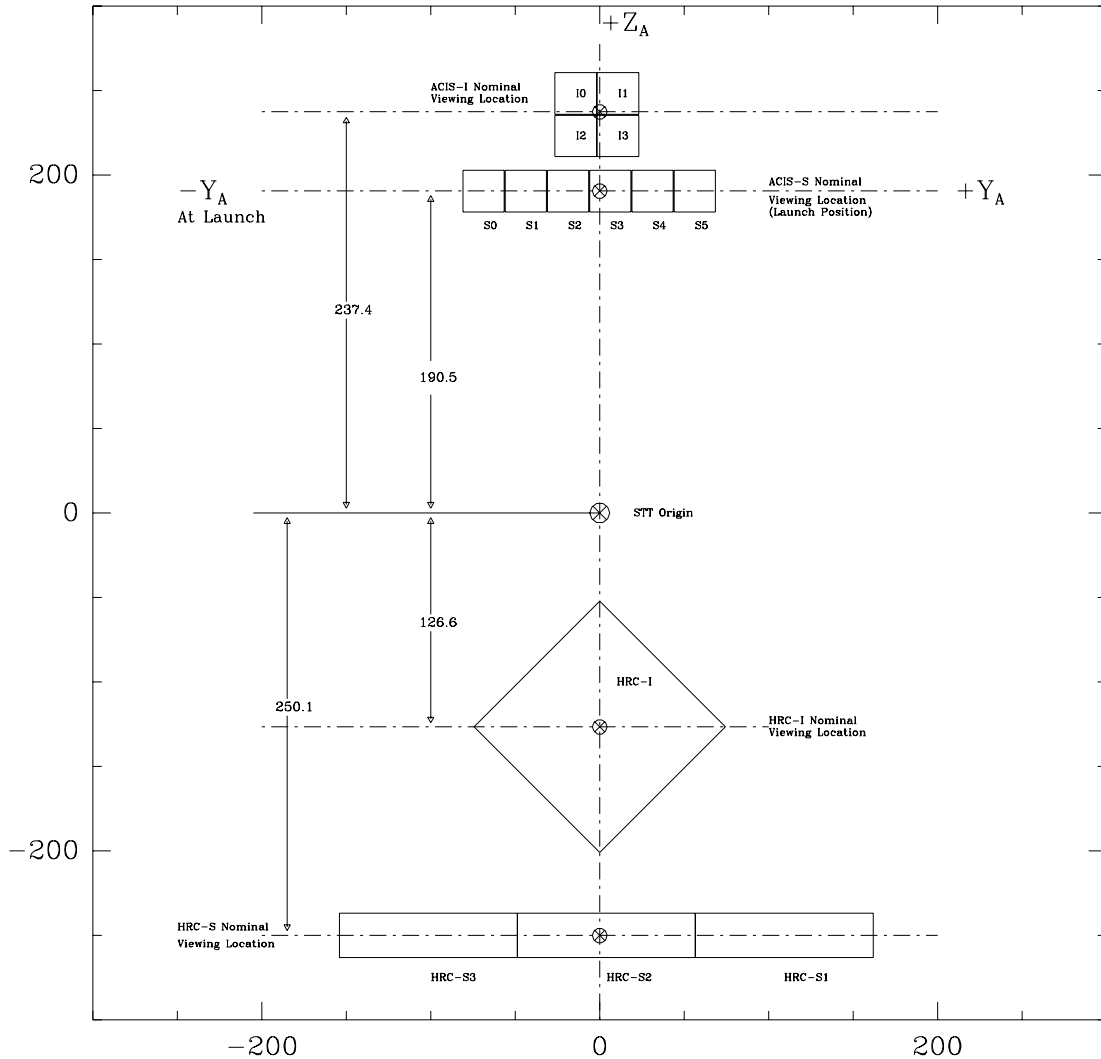

Figure 2: Chandra Detectors Layout: The schematic of the SIM plane shows the Chandra focal plane instrument to scale (in mm, coordinate system is AXAF-STT-1.0). SIM +Y is along the x-axis; SIM +Z is along the y-axis. ⊗ on each detector marks the aimpoint position with nominal SIM-Z position and zero pointing offset.

4 Aimpoint and Optical Axis Drifts

Both the aimpoint and the optical axis have been drifting in the SIM plane since the Chandra launch. Their relative positions change continuously. Their positions on each detector are critical for the optimal operation of the Chandra X-ray Observatory. Therefore the positions of both points are continuously monitored.

4.1 Aimpoint Drift

Since launch, the Chandra aimpoint has been drifting in the SIM [−Y,−Z] direction. Figures 3 − 6 show the aimpoint (with zero offset) positions of all the Chandra observations with nominal SIM-Z positions and without gratings, on all four detectors in chip coordinates as a function of time since launch. It is seen that the aimpoint has been drifting in the SIM [−Y,−Z] direction from 1999 until the beginning of year 2011. During that period, there are two relatively large shifts in June 2003 and November 2006, which are due to the ACA cool-down. Then in early 2011, the aimpoint drift reversed its direction, especially after the safemode in July 2011. In early 2012, the aimpoint drift is reversed again, back to its original trend in the SIM [−Y,−Z] direction, and the drifting rate has accelerated since. Note also the trend of increasing short-term fluctuations of the aimpoint position, presumably due to the decreasing thermal stability in the ACA housing.

4.2 Optical Axis Drift

Unlike the aimpoint, the drift of the optical axis does not exhibit any particular trend. The optical axis position is derived from data obtained on annual raster scan observations of Ar Lac, an eclipsing RS CVn binary star, with the HRC-I. Raster scan is a set of 21 observations with a 3 ks on-axis exposure and 20 1 ks off-axis exposures, with offsets ranging from $2.00'$ to $14.14'$. As the observations go off-axis, their image encircled energy radii become larger and larger. The optical axis is determined by fitting the encircled energy radii of the central 17 raster scan observations (the on-axis exposure and 16 off-axis exposures, with the largest offset at $6.00'$) to a 2-dimensional quadratic function in detector coordinates.

Figure 7 shows the central 17 raster scan data points taken in September 2014. The five circles around each data point indicate the 50%, 60%, 70%, 80% and 90% encircled energies. For clarity, the circle radii are 5 times the actual encircled energy radii. The optical axis is determined by fitting the these 17 encircled energy radii to a 2-dimensional quadratic function in detector coordinates. By definition, the optical axis is at the point where the quadratic function is at its minimum. Figure 8 shows the optical axis derived from the above 2-D quadratic fit using the September 2014 data. Figure 9 shows all the optical axis positions so determined since the Chandra launch. It moves like a random walk but is relatively stable. Its movement is well within a $10''$ region. Since year 2000, the optical axis drift was only in a $6''$ region.

The HRC-I is the only detector for which the optical axis is directly measured.
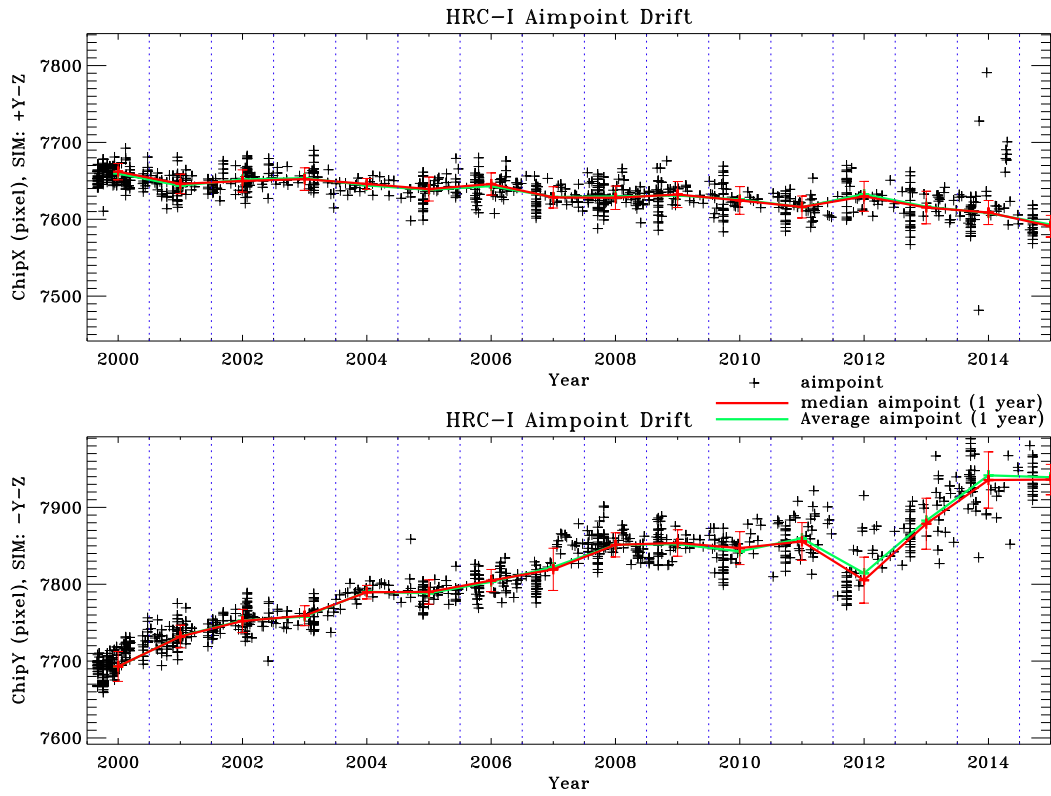
Figure 3: Aimpoint position as a function of time on HRC-I. Solid red (green) lines show the median (average) aimpoint drift in one year bins, separated by vertical dotted blue lines.
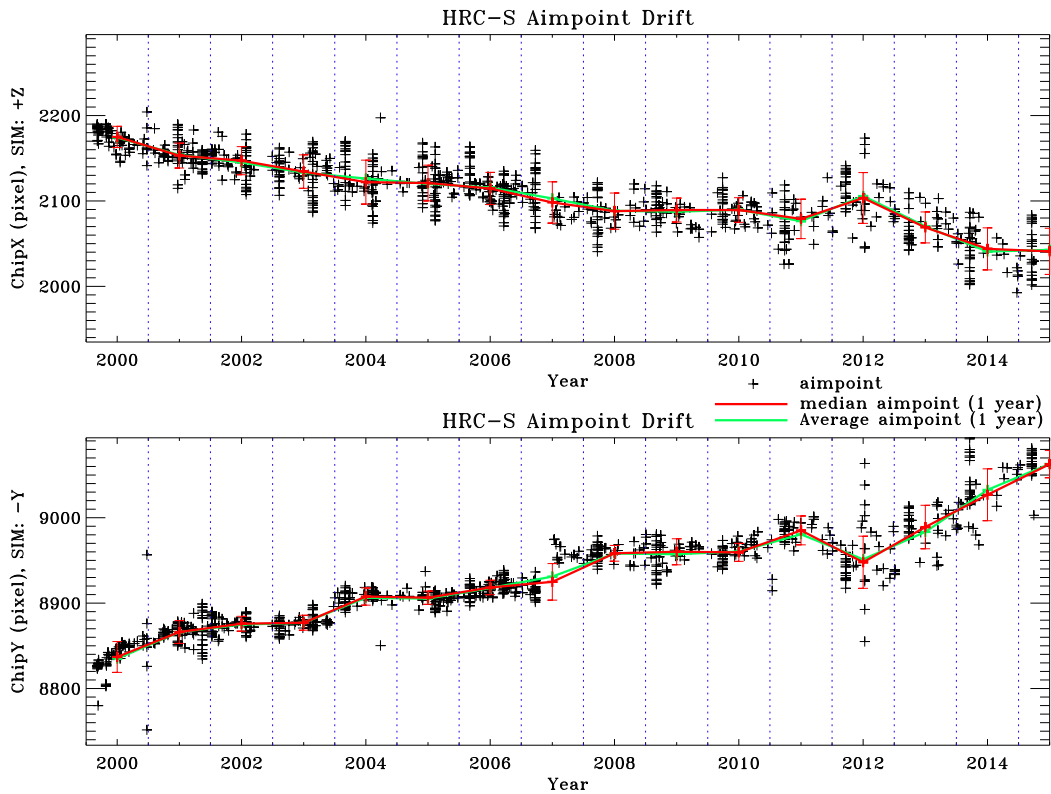

Figure 4: Aimpoint position as a function of time on HRC-S. Solid red (green) lines show the median (average) aimpoint drift in one year bins, separated by vertical dotted blue lines.
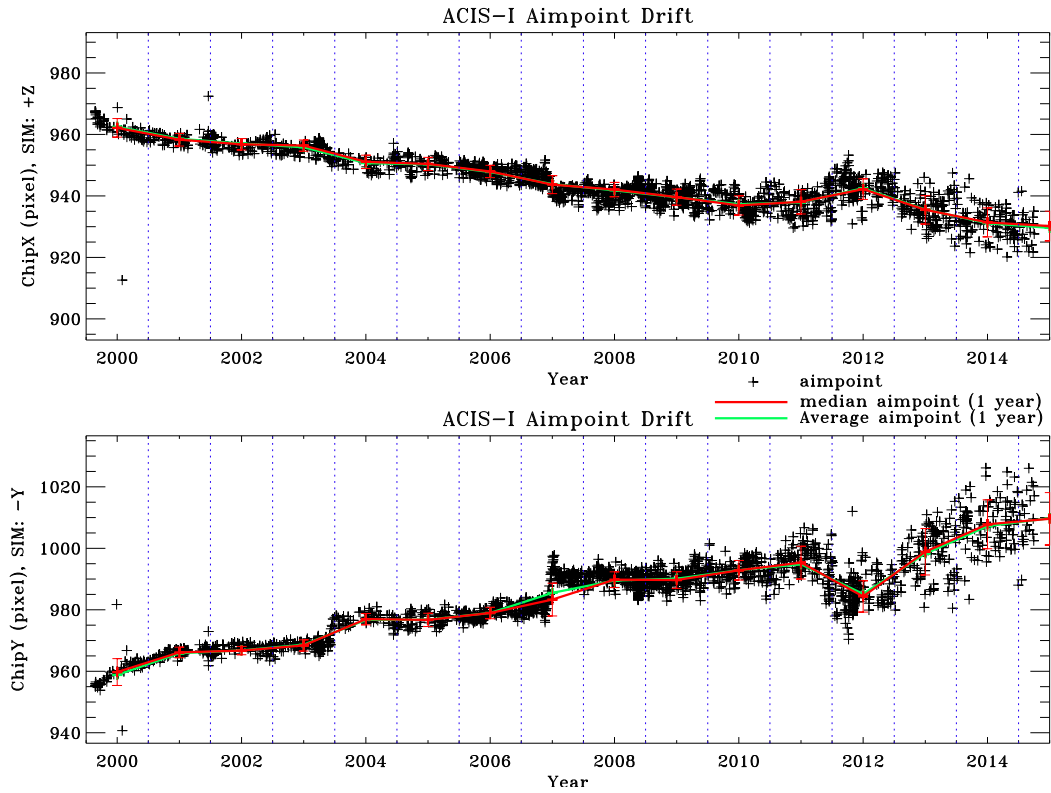
Figure 5: Aimpoint position as a function of time on ACIS-I. Solid red (green) lines show the median (average) aimpoint drift in one year bins, separated by vertical dotted blue lines.
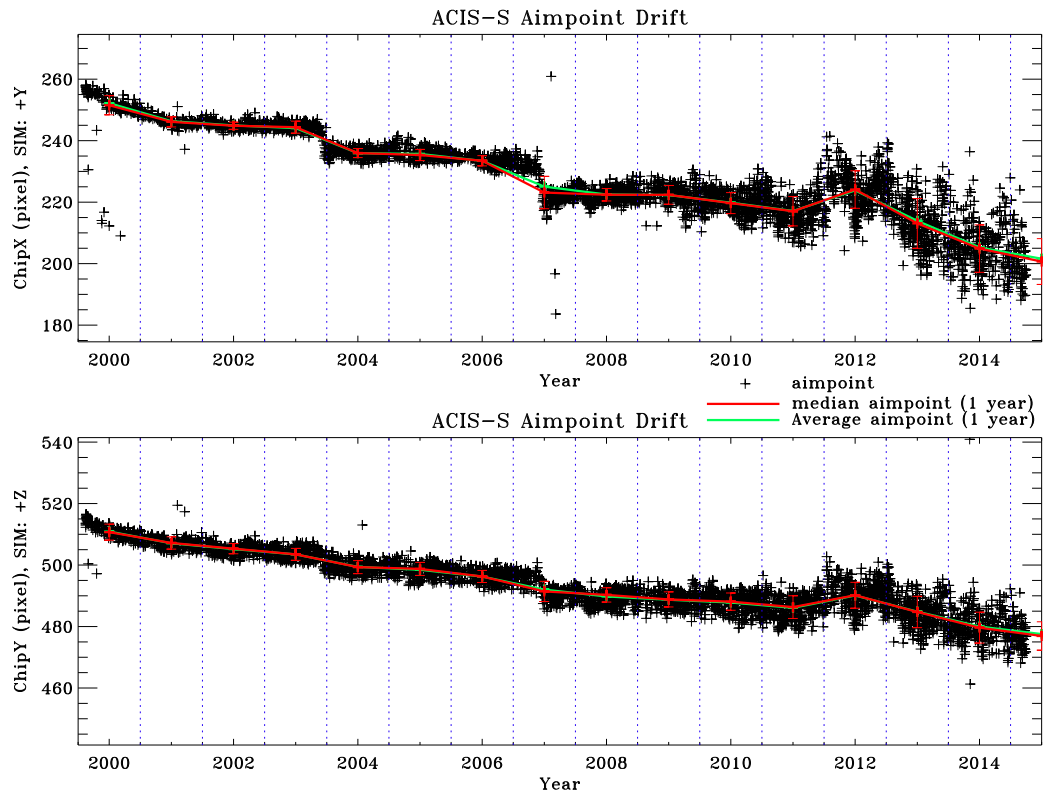

Figure 6: Aimpoint position as a function of time on ACIS-S. Solid red (green) lines show the median (average) aimpoint drift in one year bins, separated by vertical dotted blue lines.
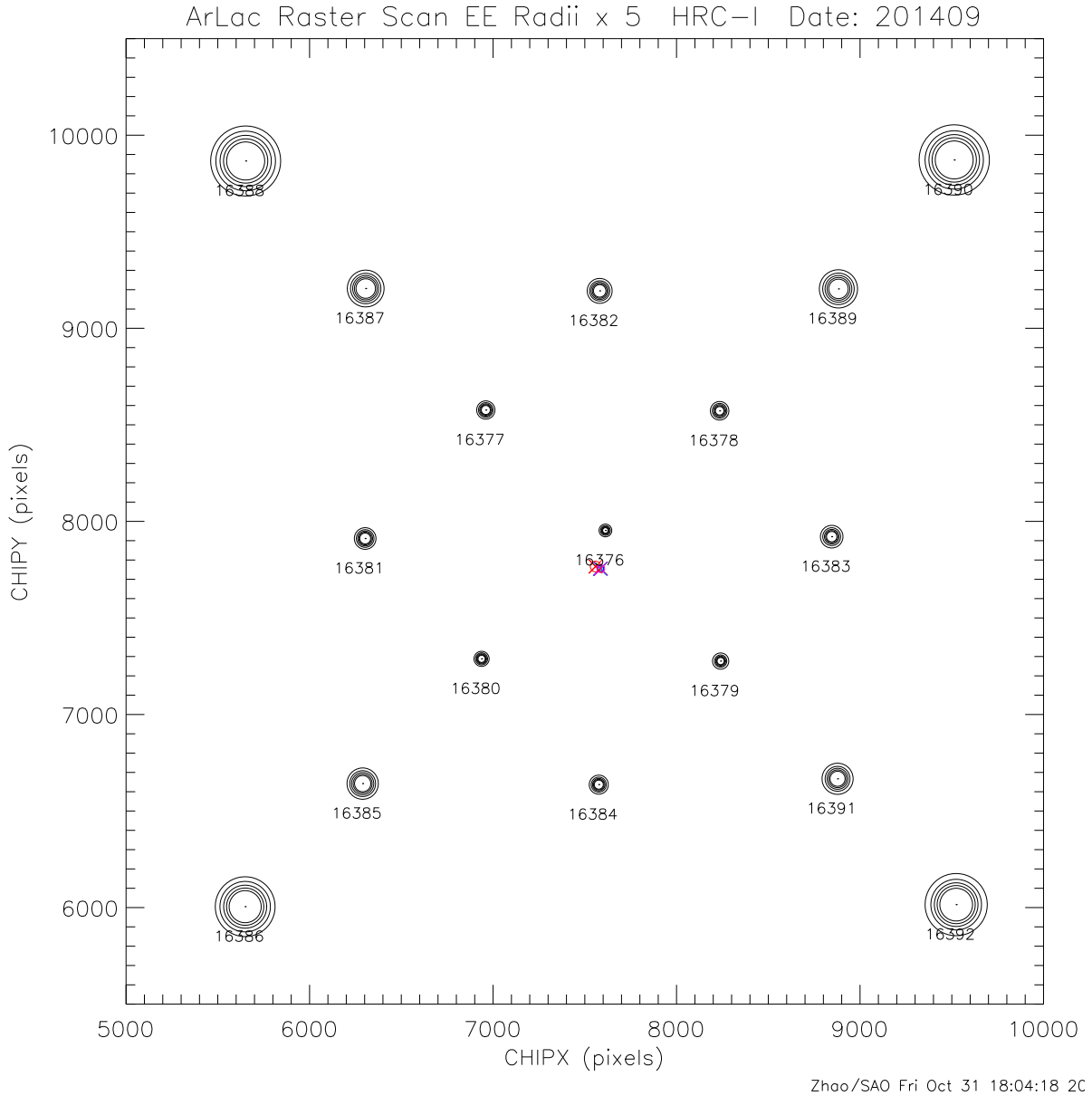
Figure 7: HRC-I raster scan observation of Ar Lac in chip coordinates. Circles around each observation point have the 50% – 90% encircled energy radii × 5. The data are fit to a 2-D quadratic function to find the optical axis. Data taken in September 2014. The numbers under the circles are the OBSIDs of the observations.
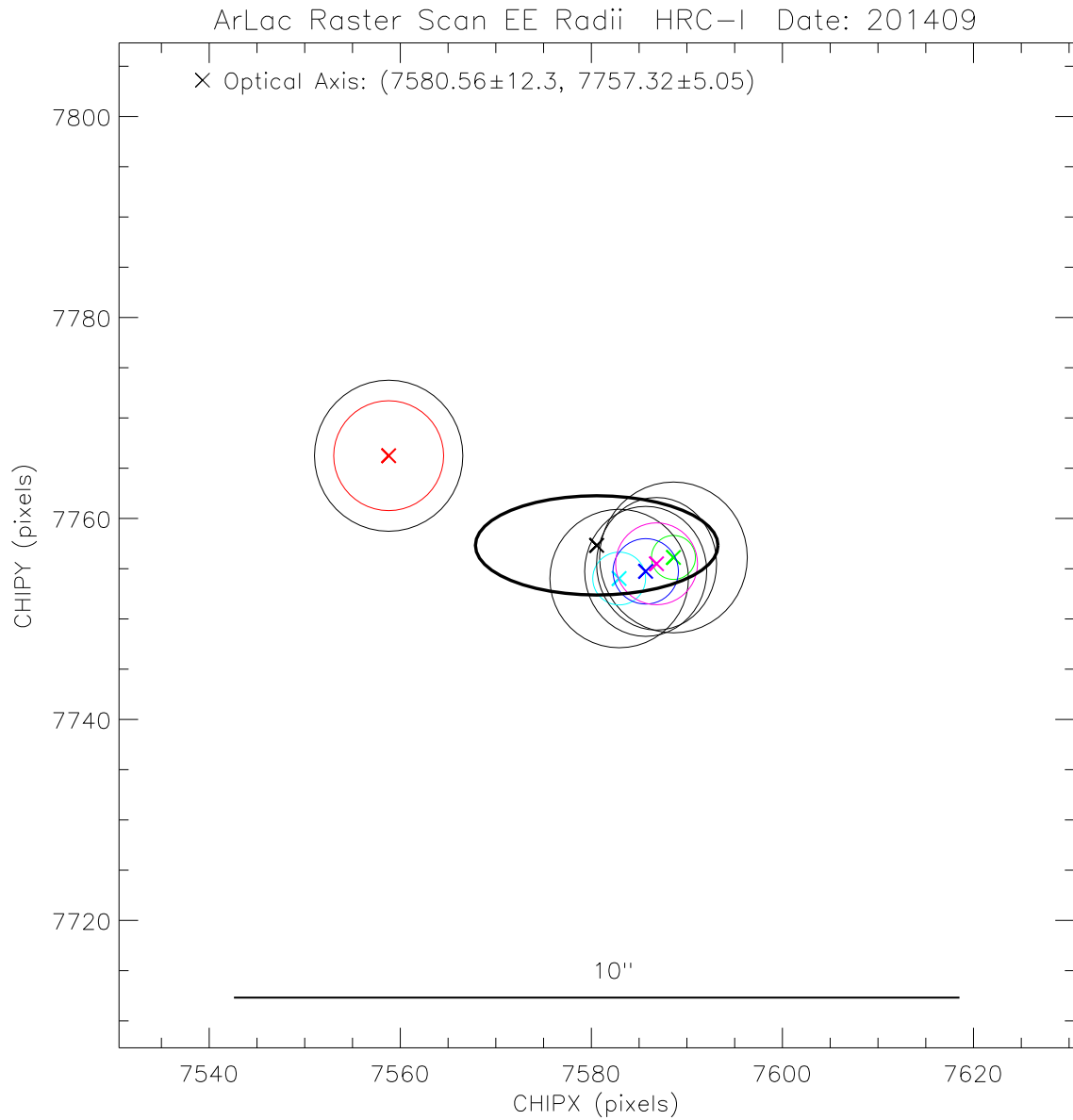
Figure 8: Same as Fig. 7 but zoomed in to the optical axis region. The five colored ×'s are the positions of quadratic function minimum for 50% – 90% encircled energy fit. The colored circles indicate their encircled energy radii. The black circles are the 1-σ fit errors. The black × marks the optical axis position, taken as the mean of the above 5 minimums. The black oval is the 1-σ error ellipse.
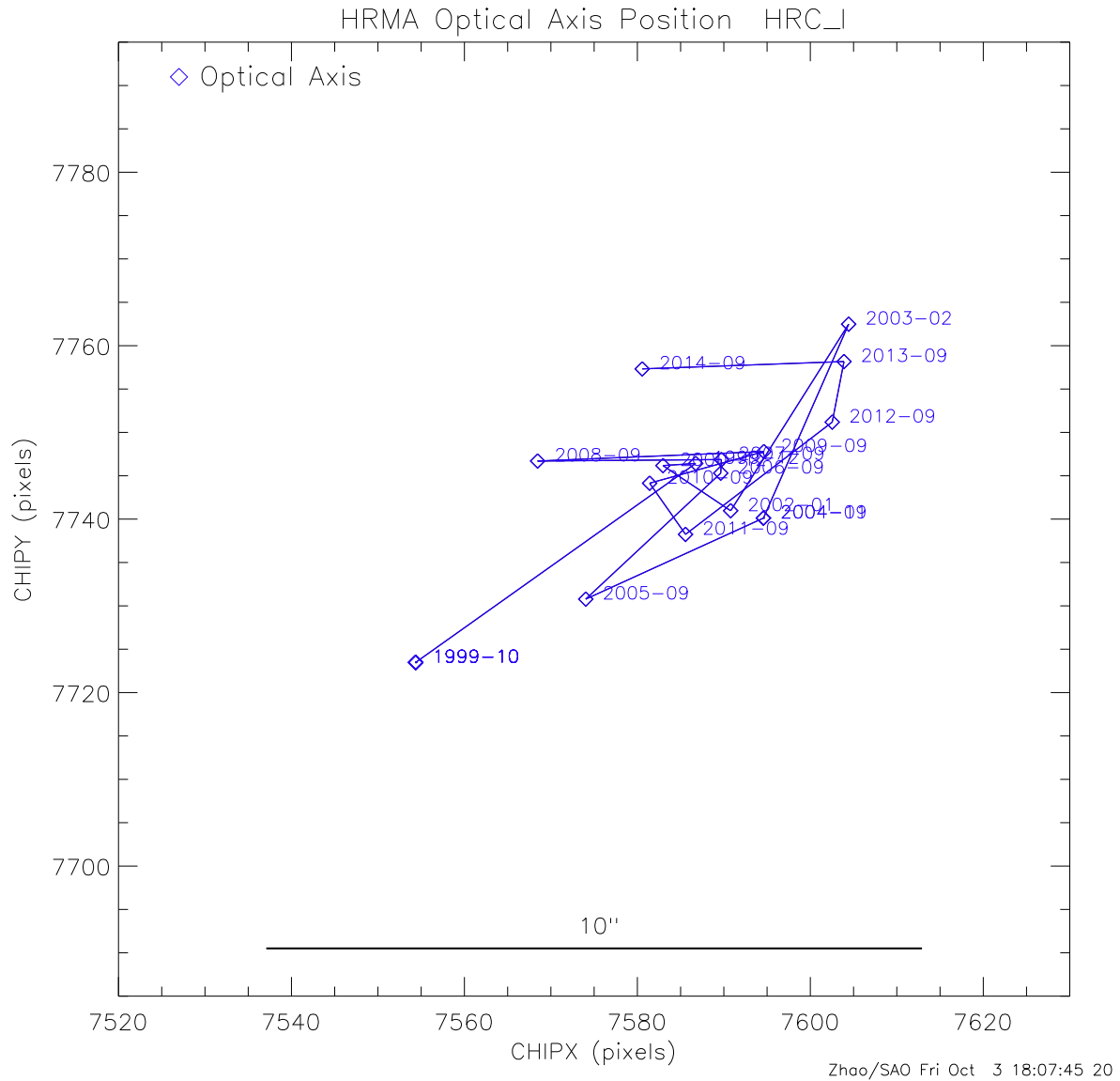
Figure 9: Chandra optical axis positions on HRC-I since launch. Each position is labeled by the year–month. The position is relatively stable and well with in a $10''$ region. Since year 2000, the optical axis drift was only in a $6''$ region.

5   Aimpoint and Optical Axis on Detectors

Aimpoint positions are measured on all four detectors as described in Section 4.1. The optical axis positions are measured only on HRC-I as described in Section 4.2. However, at any given time, the relative position between the aimpoint and optical axis is the intrinsic property of the HRMA and ACA, independent of the detectors. One can therefore calculate the optical axis position on other detectors based on its relative position to the aimpoint.

Figures 10 and 11 show the optical axis and aimpoint positions on HRC-I and HRC-S. The blue diamonds show the optical axis positions. The red arrows show the aimpoint position drift. While the optical axis is relatively stable, the aimpoint has been drifting in the SIM [−Y,−Z] direction since the Chandra launch until early 2011, for about 24″. Then it reversed its drift direction, especially after the safemode in July 2011. In early 2012, the aimpoint drift is reversed again, back to its original trend in the SIM [−Y,−Z] direction, and the rate of drift has accelerated.

Figure 12 shows the optical axis and aimpoint positions on ACIS-I. The aimpoint positions are measured directly on ACIS-I. The optical axis positions are calculated based on their relative positions to the aimpoint from HRC-I. The green arrows in the Figure indicate the default offsets applied to avoid the on-axis target falling off the ACIS-I3 edge during the dither (see Section 6 for more details). The ACIS-I observations were conducted without default offset since launch until late 2006. Due to the aimpoint drifting, from December 2006 to December 2013, all the ACIS-I observations were conducted with a default offset of Y-offset $= -15''$ and Z-offset $= -12''$, unless the observers requested otherwise. Due to its accelerated drift since early 2012, the aimpoint was once again very close to the upper edge of the ACIS-I3 in late 2013. So since December 2013, a new default offset of Y-offset $= -18''$ and Z-offset $= -18''$ was applied, as shown in Figure 12. In the past year, the aimpoint continued to drift towards the ACIS-I3 chip edge. But it did not drift far enough to warrant another new default offset. So it is still safe to operate the ACIS-I with the current default offset, [$-18''$, $-18''$], for Cycle 17 (see Figure 12).

Figure 13 shows the optical axis and aimpoint positions on ACIS-S. The aimpoint positions are measured directly on ACIS-S. The optical axis positions are calculated based on their relative positions to the aimpoint from HRC-I. Because of the aimpoint drift, four different default offsets have been implemented between August 1999 and August 2011, in order to avoid the dither pattern falling on the node boundary 0|1. These are indicated by the green arrows in the figure (see Section 6 for more details). Due to its accelerated drift since early 2012, the aimpoint moved far enough from the node boundary 0|1. So since December 2013, a fifth default offset of Y-offset $= 0''$ and Z-offset $= -18''$ was applied, to move the aimpoint closer to the optical axis, as shown in Figure 13. In the past year, the aimpoint continued to drift away from the node boundary 0|1. But it is still reasonably close to the optical axis ($\sim 15''$ with the current default offset). So it is still safe to operate the ACIS-S with the current default offset, [$0''$, $-18''$], for Cycle 17 (see Figure 12).

Figure 14 shows the four figures the same as Figures 10 – 13 and with colored ovals indicating the 1-σ error ellipse for data in a given 1-year bin.

Figure 15 is the same as Figure 14 and with colored dots showing the aimpoints of individual observations.

Figure 16 shows the four figures the same as Figures 10 – 13, but with the same SIM coordinate orientation (SIM-Z up, SIM-Y right, refer Figure 2). It shows the relative positions of the optical axis (blue) and the the aimpoint (red). It also shows the aimpoints drifted in the same direction on the four detectors.
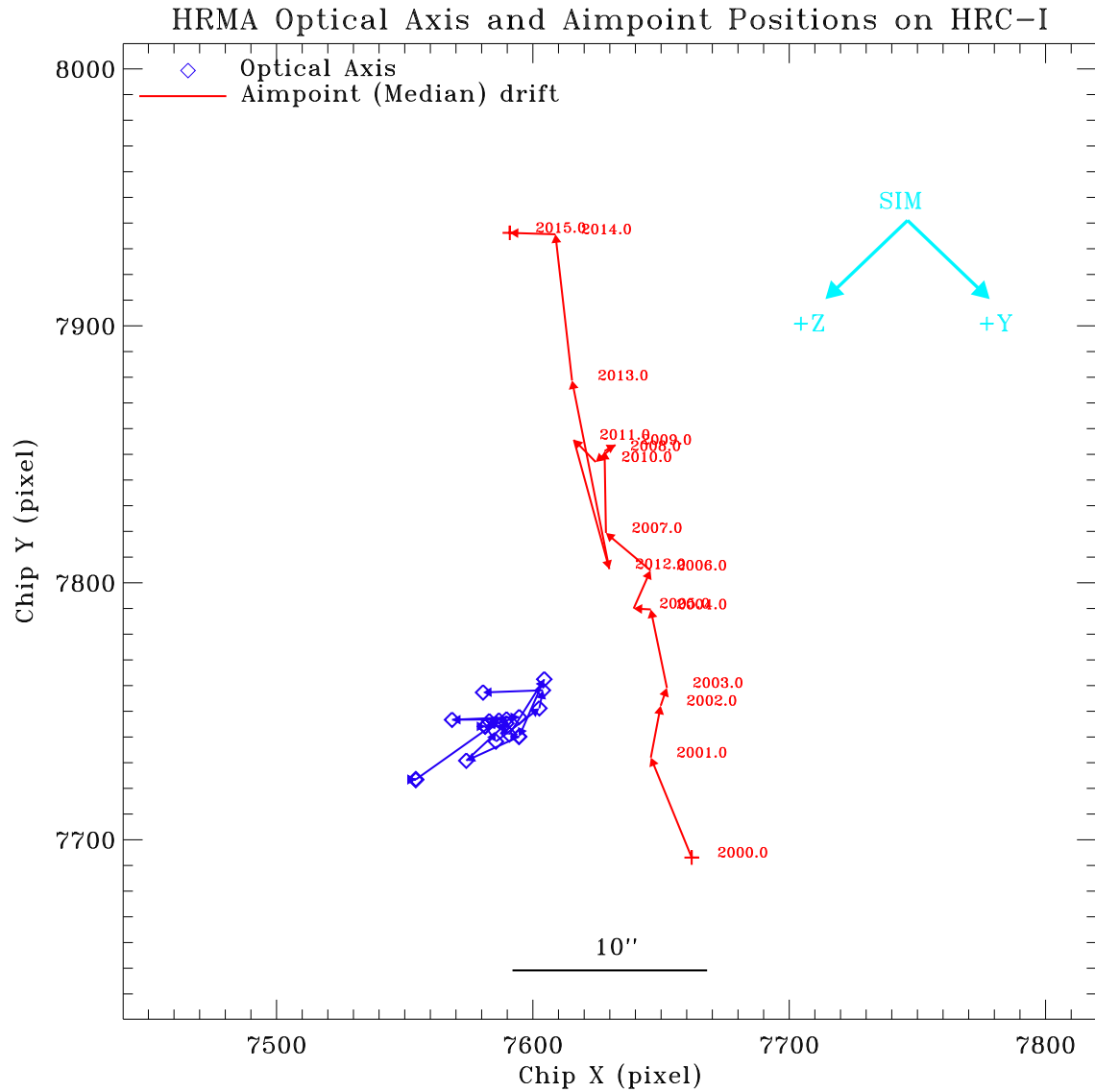
Figure 10: Chandra optical axis (blue) and median aimpoint (red, see Fig. 3) position for each year on HRC-I. Each aimpoint position is labeled by the year. The cyan colored arrows show the SIM coordinates.

Figure 11: Chandra optical axis (blue) and median aimpoint (red, see Fig. 4) position for each year on HRC-S. Each aimpoint position is labeled by the year. The cyan colored arrows show the SIM coordinates.

Figure 12: Chandra optical axis (blue) and median aimpoint (red, see Fig. 5) position for each year on ACIS-I. Each aimpoint position is labeled by the year. The cyan col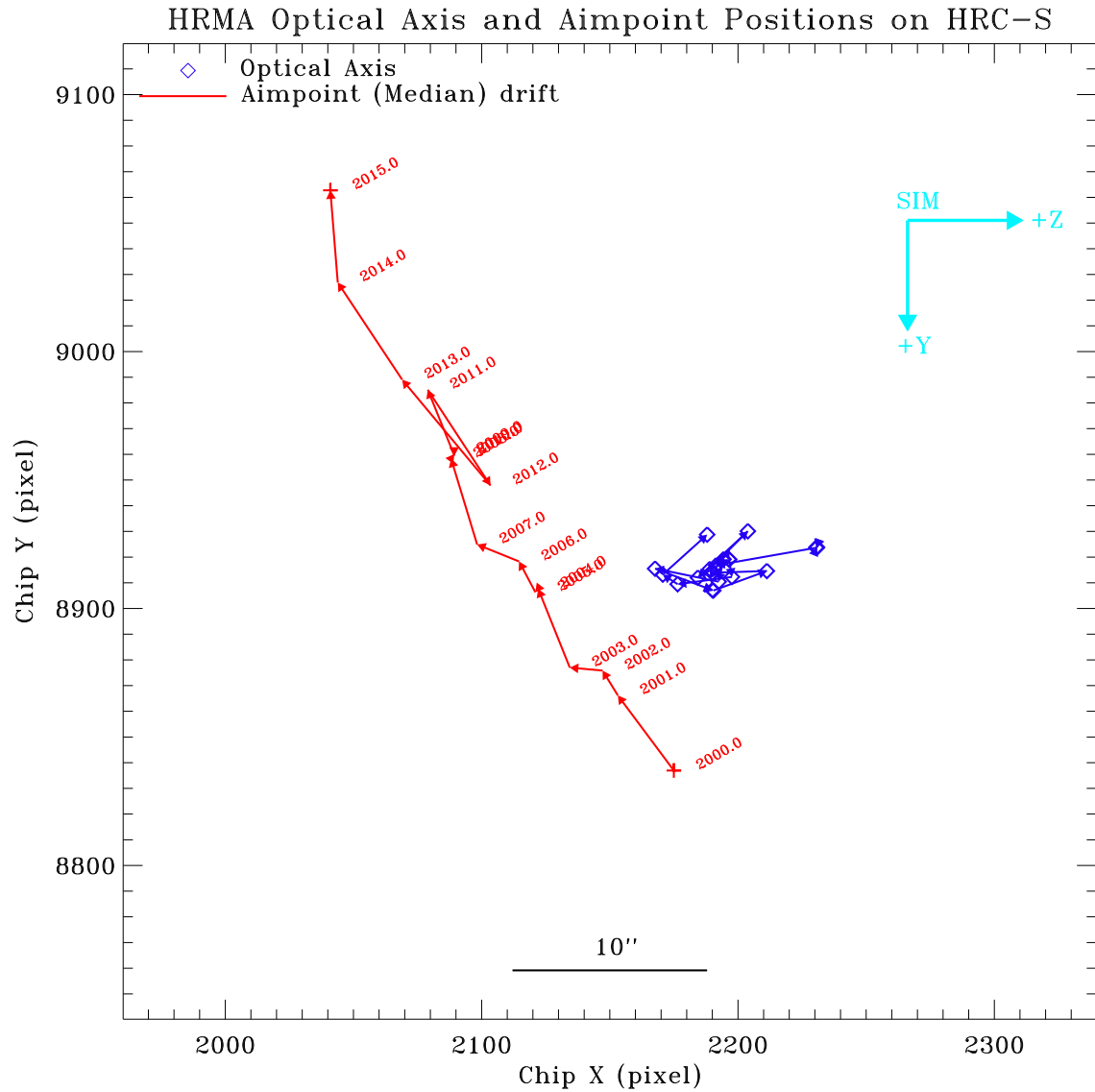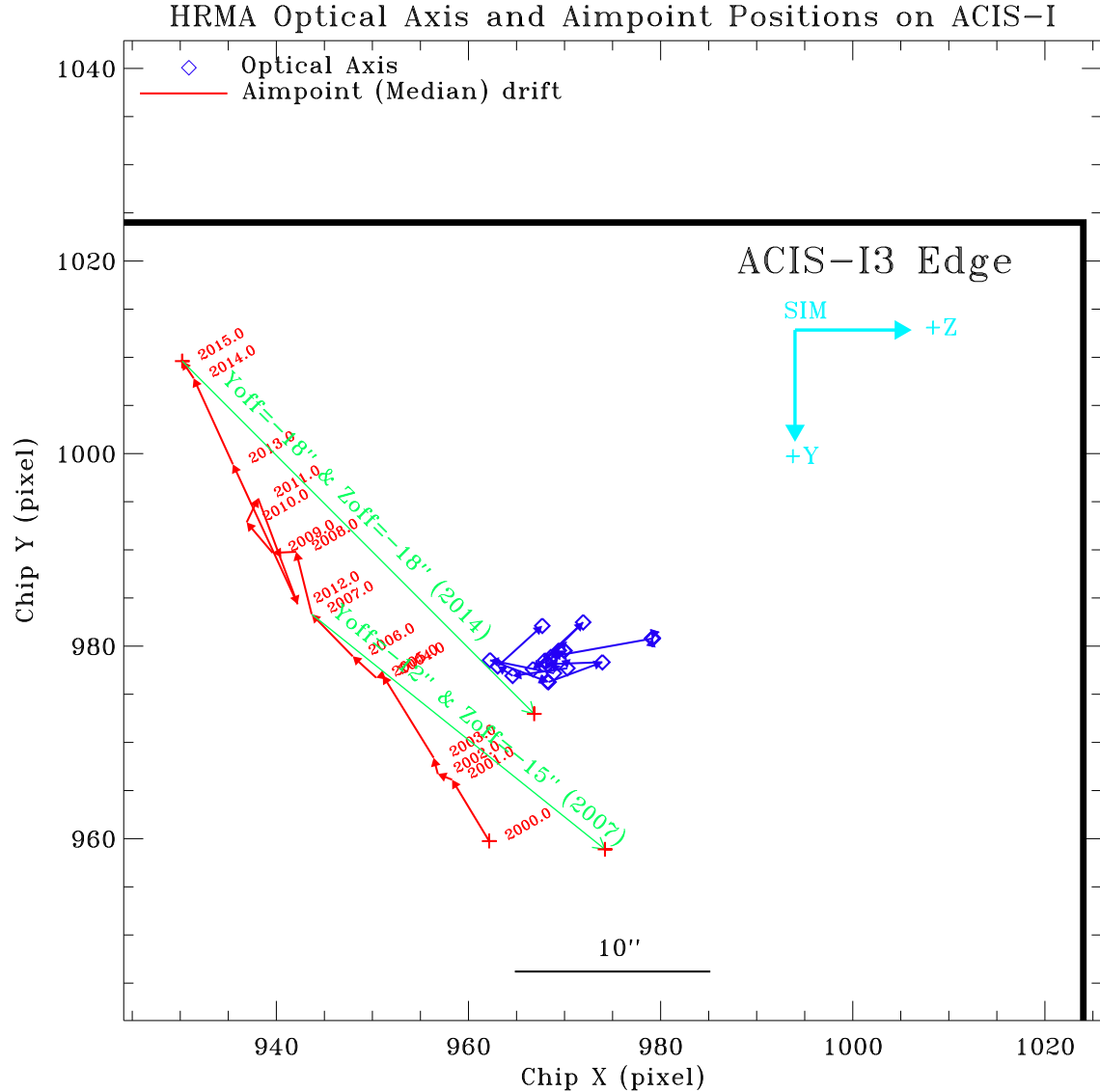ored arrows show the SIM coordinates. ACIS-I observations were conducted without default offset since the Chandra launch until the end of 2006. In December 2006, the aimpoint had a sudden shift of $\sim 10''$ due to the ACA primary focal plan CCD cool down from $-15°$C to $-20°$C. This sudden shift brought the aimpoint uncomfortably close to the ACIS-I3 chip edge. As it continue to drift towards the edge, the dither pattern ($16''$ peak-to-peak) will soon fall out of the chip. Therefore a default Y-offset $= -15''$ and Z-offset $= -12''$ was implemented to move the aimpoint away from the chip edge and also closer to the optical axis. Due to its accelerated drift since early 2012, the aimpoint was once again very close to the ACIS-I3 edge in late 2013. So since December 2013, a new default offset of Y-offset $= -18''$ and Z-offset $= -18''$ was applied. The two green arrows in the figure show the magnitude and the direction of the default offsets. All the ACIS-I observations were conducted with these default offsets starting in the year labels next to the green arrows, unless the observers requested otherwise.

Figure 13: Chandra optical axis (blue) and median aimpoint (red, see Fig. 5) position for each year on ACIS-S. Each aimpoint position is labeled by the year. The cyan colored arrows show the SIM coordinates. The green arrows show the default offsets implemented over the years (see Section 6 for more details). The current default offset is Y-offset $= 0''$ and Z-offset $= -18''$, implemented in December 2013. All the ACIS-S observations were conducted with these default offsets starting in the year labels next to the green arrows, unless the observers requested otherwise.
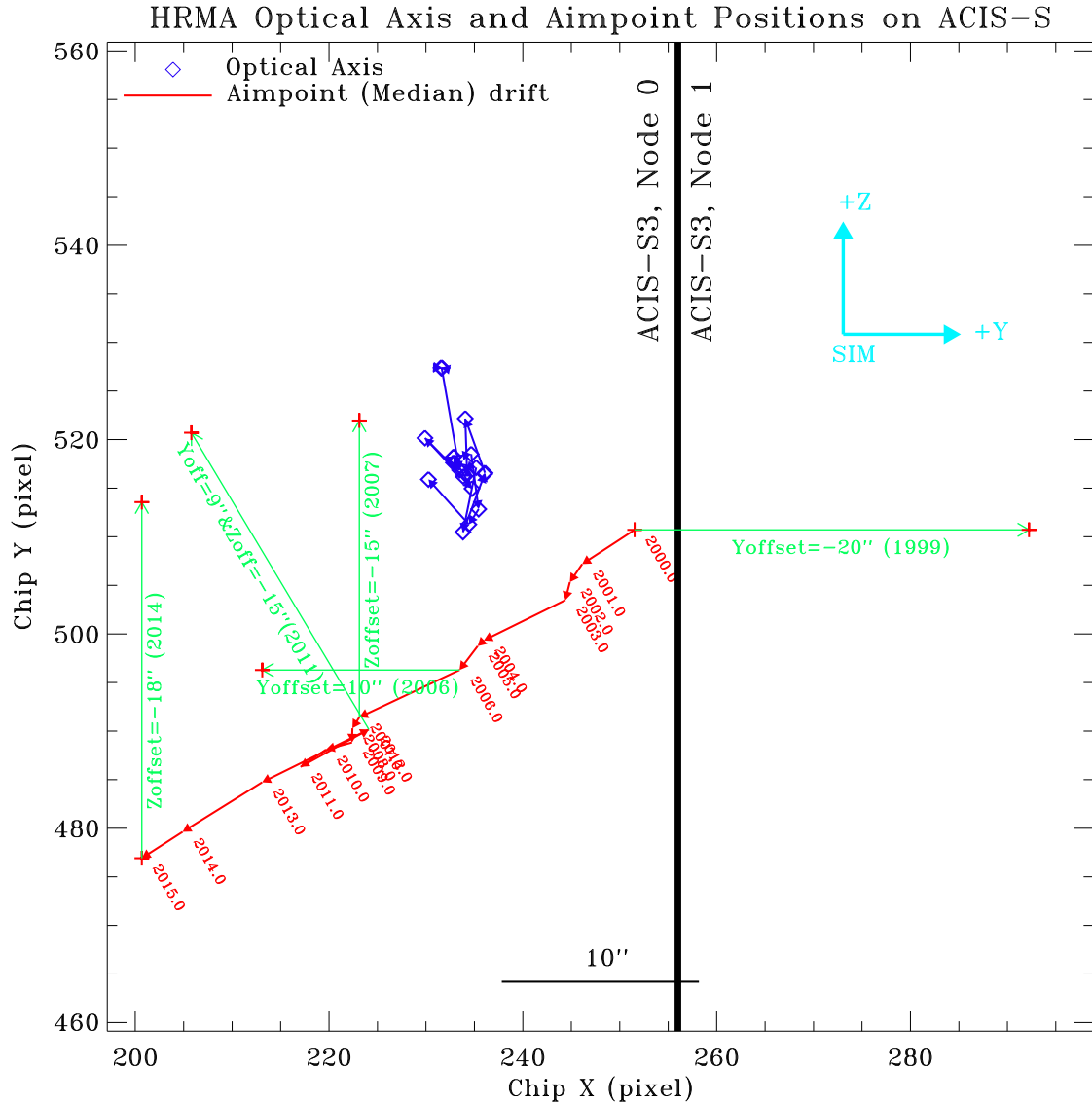
Figure 14: Same as Figures 10 – 13, the optical axis (blue) and median aimpoint (red) drifts on HRC-I (upper-left), HRC-S (upper-right), ACIS-I (lower-left) and ACIS-S (lower-right), with the colored ovals indicating the 1-σ error ellipse for data in a given 1-year bin.

Figure 15: Same as Figures 14, the dots near the ovals of the same color are the aimpoints of individual observations for that given year.

Figure 16: Same as Figures 10 – 13, but with the same SIM coordinate orientation (SIM-Z up, SIM-Y right, refer Figure 2). The aimpoints (red) drift in the same direction on HRC-I (upper-left), HRC-S (upper-right), ACIS-I (lower-left) and ACIS-S (lower-right).

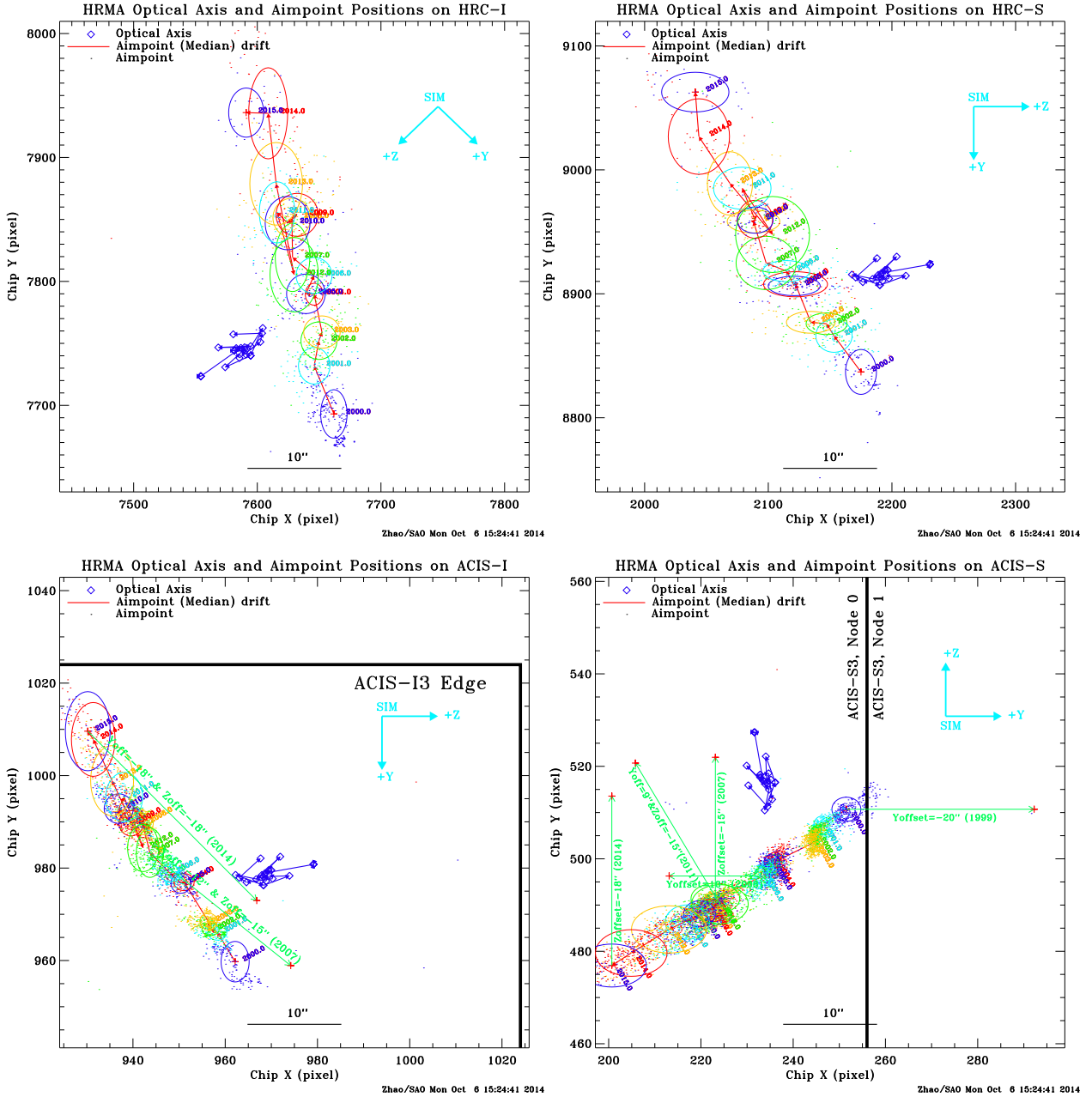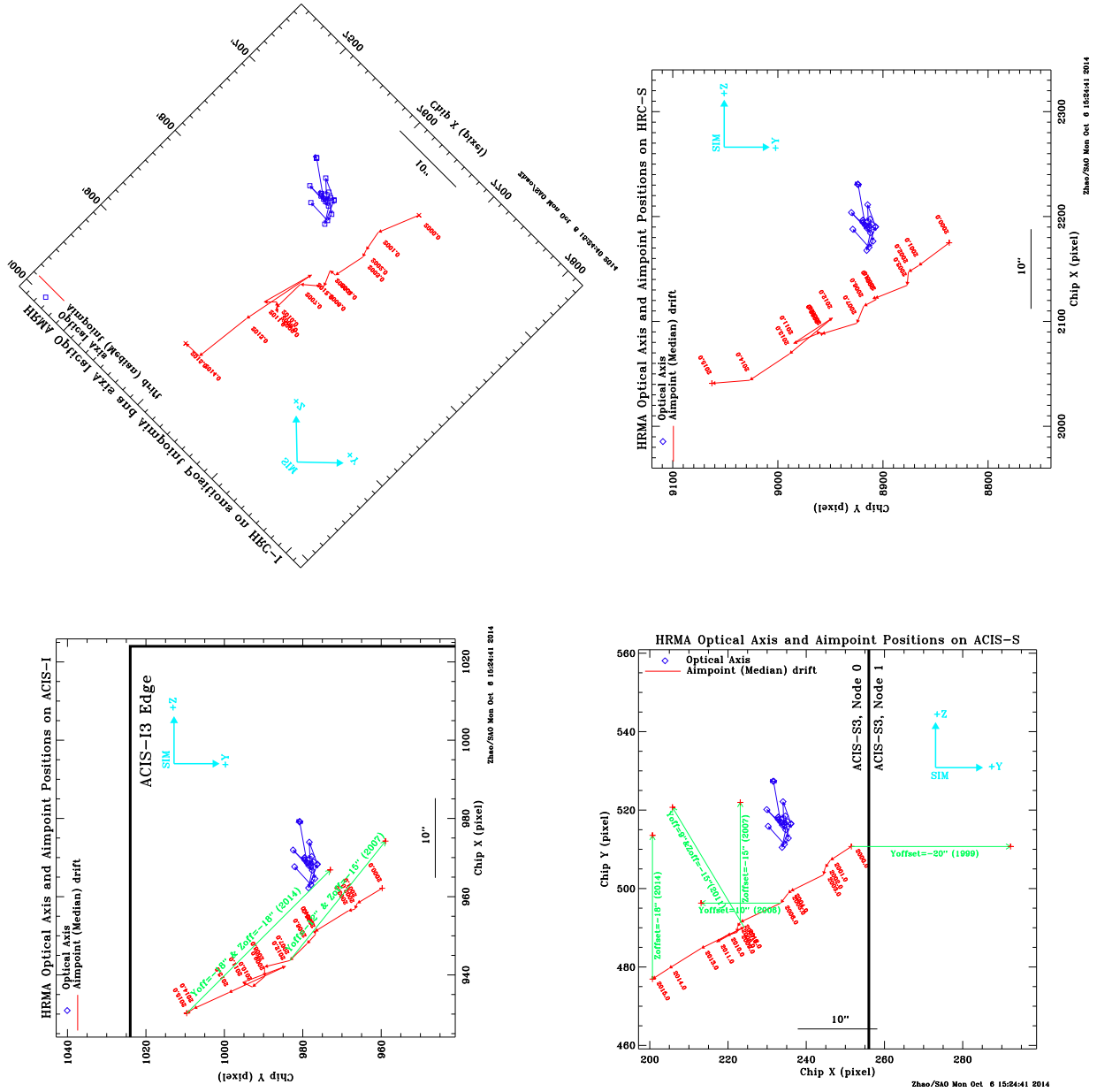## 6   Aimpoint Default Offsets

It is not desirable for the aimpoint to be too close to the edge of an ACIS chip or node boundary. In order to avoid the dithered image of on-axis targets falling off the edge or crossing the node boundary, default pointing offsets were applied on ACIS detectors. Since the aimpoint has been drifting, the default offset has been adjusted accordingly during the course of the Chandra operation. Table 1 summarizes these default offset implementations on ACIS-I and ACIS-S since the Chandra launch. They are illustrated in Figures 12 and 13 with green arrows. The latest, and current, default offsets were applied in Dec. 2013.

Table 1: Default Offsets from Aimpoint on ACIS Detectors

Detector	Date Applied	Y-offset	Z-offset	Reason
ACIS-I	1999 Aug.	$0''$	$0''$	No offset needed.
	2006 Dec.	$-12''$	$-15''$	Move the aimpoint away from the I3 edge & closer to optical axis.
	2013 Dec.	$-18''$	$-18''$	Move the aimpoint away from the I3 edge & closer to optical axis.
ACIS-S	1999 Aug.	$-20''$	$0''$	Move the aimpoint away from node 0|1
	2005 Dec.	$+10''$	$0''$	Move the aimpoint away from node 0|1
	2006 Dec.	$0''$	$-15''$	Move the aimpoint closer to optical axis.
	2011 Aug.	$+9''$	$-15''$	Move the aimpoint away from node 0|1 & closer to the optical axis.
	2013 Dec.	$0''$	$-18''$	Move the aimpoint closer to optical axis.

The aimpoints on HRC-I and HRC-S are well within the center regions of both detectors. Thus there are no default offset ever needed for HRC detectors.

7   Impact on Chandra Observations

Because the optical axis position has been relatively stable (as shown in Section 4.2), the HRMA PSF and therefore the superb Chandra imaging resolution has always been the same since the Chandra launch.

Given the aimpoint has been drifting and appropriate default offsets have been implemented to compensate the drift (see Section 6), the relative positions of the optical axis and aimpoint has been changing, but at no time they were more than $27''$ apart. Since this is relatively small comparing to the offaxis angle at which the PSF starting to degrade (See POG Figures 4.12 and 4.13), the PSF of near axis sources has always stayed the same during the entire Chandra operation.

8   Current Optical Axis and Aimpoint positions

Each October, a new table of optical axis and aimpoint positions are compiled for the new release of Chandra POG (Proposers' Observatory Guide), CIAO (Chandra Interactive Analysis of Observations) and ObsVis (The Chandra Observation Visualizer).

Based on the current measurements, the predicted Chandra Cycle 17 optical axis and median aimpoint position and their standard deviation (σ) are listed in Table **??**. On-axis targets will be imaged at the aimpoint (with the default offsets for ACIS-I and ACIS-S) chip coordinates on each detector. Observers should use this table to check their target location and may request different pointing offset based on their sources to maximize the scientific return. If the observer do not request a specific pointing offset, the default offset will be applied. Table **??** can also be found at `http://cxc.harvard.edu/cal/Hrma/OpticalAxisAndAimpoint.html`.

Table 2: Chandra Optical axis and aimpoint Positions for Cycle 17

Detector	SIM-Z (mm)	Optical Axis (pixel) ChipX(σ)	ChipY(σ)	Aimpoint (pixel) ChipX(σ)	ChipY(σ)	Chip	Default offset [ΔY,ΔZ]
ACIS-I	-233.587	967.7(2.5)	982.1(2.5)	930.2(4.8)	1009.6(8.5)	I3	none
				966.8(4.8)	973.0(8.5)	I3	$[-18'',-18'']$
ACIS-S	-190.143	230.3(2.5)	515.9(2.5)	200.7(7.5)	476.9(4.6)	S3	none
				200.7(7.5)	513.5(4.6)	S3	$[0'',-18'']$
HRC-I	126.983	7580.6(12.4)	7757.3(5.1)	7591.0(14.1)	7936.1(19.8)		none
HRC-S	250.466	2188.0(9.4)	8928.8(9.4)	2041.0(27.1)	9062.7(15.9)		none

9 Summary

By studying the optical axis and aimpoint, we can understand the long term stability and imaging quality of the telescope and ensure its optimal performance.

The study shows that optical axis position has been relatively stable since the Chandra launch. Its random walk like movement is well within a $10''$ region, and within a $6''$ region since year 2000. This result indicates that the HRMA, optical bench and SIM are all very rigid and stable. Therefore the superb Chandra spatial resolution has always been the same.

The study shows that the aimpoint has been drifting in the SIM $[-Y,-Z]$ direction for about $30''$ since launch. Since 2011 the drift has reversed its direction twice and the rate of drift has accelerated. In addition, the short term fluctuation has gradually increased. The aimpoint drift is caused by the alignment change between the ACA and the HRMA. Its long term change is due to the aging and relaxing of the material. Its short term change is usually associated with the thermal change in the ACA housing. So in order to keep the aimpoint stable in short term, we need to keep a constant temperature of the ACA.

The latest default offsets on both ACIS-I and ACIS-S were implemented in December 2013. In the past year, the aimpoint drifted in the same direction as in the previous two years. But it is still safe to operate with the current default offsets. Therefore this memo recommends to keep the current default offsets of ACIS-I and ACIS-S for Chandra Cycle 17.

Although both optical axis and aimpoint have been drifting since the Chandra launch, at no time Chandra's imaging quality was compromised. We just need to continue monitoring their drifts and adjust the default pointing offsets to avoid the aimpoint getting too close to the chip edge or the node boundary.

This memo can be found at:
`http://cxc.harvard.edu/cal/Hrma/rsrc/Publish/Optics/OpticalAxisAndAimpoint/oxap_memo_2014.pdf`

References

[Zhao (2004)] Zhao, Ping "Chandra Telescope Optical Axis", Chandra Calibration Workshop, 2004, Cambridge, MA
`http://cxc.cfa.harvard.edu/ccw/proceedings/04_proc/presentations/zhao`

[Zhao (2005)] Zhao, Ping "Chandra Telescope Optical Axis and Aimpoint", Chandra Calibration Workshop, 2005, Cambridge, MA
`http://cxc.cfa.harvard.edu/ccw/proceedings/05_proc/presentations/zhao`

[Zhao (2006)] Zhao, Ping "Chandra Telescope Optical Axis and Aimpoint", Chandra X-ray Center Memorandum, 2006
`http://cxc.harvard.edu/cal/Hrma/rsrc/Publish/Optics/OpticalAxisAndAimpoint/opt_axis_memo.pdf`

[Zhao (2007)] Zhao, Ping "Chandra Telescope Optical Axis and Aimpoint", Chandra Calibration Workshop, 2007, Huntsville AL
`http://cxc.cfa.harvard.edu/ccr/proceedings/07_proc/presentations/zhao`

[Zhao (2009)] Zhao, Ping "The Quality and Stability of Chandra Telescope Pointing and Spatial Resolution", Chandra Calibration Review, 2009 Boston, MA
`http://cxc.harvard.edu/ccr/proceedings/2009/presentations/zhao`

[Zhao (2011)] Zhao, Ping "Chandra Aimpoint Drift and Default Offsets", Chandra X-ray Center Memorandum, 2011
`http://cxc.harvard.edu/cal/Hrma/rsrc/Publish/Optics/OpticalAxisAndAimpoint/aimpoint_memo_2011`

[Zhao (2012a)] Zhao, Ping "Chandra X-ray Observatory Aimpoint and Optical Axis", `AAS 219th meeting, 2012, Bull.Am.Astro.Soc. 219, 446.01`

[Zhao (2012b)] Zhao, Ping "The Quality and Stability of Chandra Telescope Pointing and Spacial Resolution", `AAS 220th meeting, 2012, Bull.Am.Astro.Soc. 220, 122.05`

[Zhao (2012c)] Zhao, Ping "Chandra Optical Axis, Aimpoint and Their Drifts", Chandra X-ray Center Memorandum, 2012
`http://cxc.harvard.edu/cal/Hrma/rsrc/Publish/Optics/OpticalAxisAndAimpoint/oxap_memo_2012.pdf`

[Zhao (2013)] Zhao, Ping "Chandra Optical Axis, Aimpoint and Their Drifts", Chandra X-ray Center Memorandum, 2013
`http://cxc.harvard.edu/cal/Hrma/rsrc/Publish/Optics/OpticalAxisAndAimpoint/oxap_memo_2013.pdf`

[Zhao (2014a)] Zhao, Ping "Chandra X-ray Observatory Pointing and its Stability", `AAS 223th meeting, 2014, Bull.Am.Astro.Soc. 223, 109.06`

[Zhao (2014b)] Zhao, Ping "Chandra Optical Axis, Aimpoint and Their Drifts", `HEAD 14th meeting, 2014, 116.09`